

by Felix M. Gradstein¹, James G. Ogg², Alan G. Smith³, Wouter Bleeker⁴, and Lucas J. Lourens⁵

A new Geologic Time Scale, with special reference to Precambrian and Neogene

1. Geological Museum, University of Oslo, N-0318 Oslo, Norway. Email: felix.gradstein@nhm.uio.no
2. Department of Earth & Atmospheric Sciences, Purdue University, West Lafayette, Indiana 47907-1397, USA.
3. Department of Earth Sciences, Cambridge University, Cambridge CB2 3EQ, England.
4. Geological Survey of Canada, 601 Booth Str., Ottawa, Ontario K1A 0E8, Canada.
5. Faculty of Earth Sciences, Utrecht University, 3508 TA Utrecht, The Netherlands.

A Geologic Time Scale (GTS2004) is presented that integrates currently available stratigraphic and geochronologic information. Key features of the new scale are outlined, how it was constructed, and how it can be further improved. The accompanying International Stratigraphic Chart, issued under auspices of the International Commission on Stratigraphy (ICS), shows the current chronostratigraphic scale and ages with estimates of uncertainty for all stage boundaries. Special reference is made to the Precambrian part of the time scale, which is coming of age in terms of detail, and to the Neogene portion, which has attained an ultra-high-precision absolute-age calibration.

Introduction

The geologic time scale is the framework for deciphering the history of the Earth and has three components:

- (1) The international chronostratigraphic divisions and their correlation in the global rock record,
- (2) The means of measuring absolute (linear) time or elapsed durations from the rock record, and
- (3) The methods of effectively joining the two scales.

For convenience in international communication, the rock record of Earth's history is subdivided in a "chronostratigraphic" scale of standardized global stratigraphic units, such as "Ordovician", "Miocene", "*Harpoceras falciferum* ammonite Zone" or "polarity Chron C24r". Unlike the continuous ticking clock of the "chronometric" scale (measured in years before present), the chronostratigraphic scale is based on relative time units, in which global reference points at boundary stratotypes define the limits of the main formalized units, such as "Devonian." The chronostratigraphic scale is an agreed convention, whereas its calibration to absolute (linear) time is a matter for discovery or estimation.

By contrast, Precambrian stratigraphy is formally classified chronometrically, i.e. the base of each Precambrian eon, era and period is assigned an arbitrary numerical age. This practice is now being challenged (see below).

Continual improvements in data coverage, methodology, and standardization of chronostratigraphic units imply that no geologic time scale can be final. This brief overview of the status of the Geologic Time Scale in 2004 (GTS2004), documented in detail by Gradstein et al. (2004), is the successor to GTS1989 (Harland et al., 1990), which in turn was preceded by GTS1982 (Harland et al., 1982). GTS2004 also replaces the International Stratigraphic Chart 2000 of the International Commission on Stratigraphy (ICS) and UNESCO, issued four years ago (Remane, 2000).

There are several reasons why this new geologic time scale of 2004 was required, including:

- Nearly 50 of 90+ Phanerozoic stage boundaries are now defined, versus <15 in 1990;
- Stable international stage subdivisions rendered invalid about 15% of the "stage" names of 1990;
- Last 23 million years (Neogene) is orbitally tuned with 40 kyr accuracy;
- Orbital scaling has been successful in portions of the Paleocene, lower Cretaceous, lower Jurassic, and upper Triassic;
- Superior stratigraphic integration in Mesozoic has merged direct dating, seafloor spreading (M-sequence), zonal scaling and orbital tuning;
- Superior stratigraphic scaling of Paleozoic was achieved using high-resolution composite zonal standards;
- A 'natural' geologic Precambrian time scale has been proposed to replace the current artificial scale;
- More accurate and precise age dating has provided over 200 Ar/Ar and U/Pb dates with external (systematic) error analysis, of which only a few of these were available to GTS89;
- Improved mathematical/statistical techniques can combine biostratigraphic zones, polarity chrons, geologic stages and absolute ages to calculate the linear time scale and estimate uncertainty.

A listing is provided at the end of this document of outstanding issues that, once resolved, will pave the way for an updated version of the standard Geologic Time Scale, scheduled under the auspices of ICS for the year 2008.

Overview of construction of GTS2004

Since 1989, there have been major developments in time scale research, including:

- (1) Stratigraphic standardization through the work of the International Commission on Stratigraphy (ICS) has greatly refined the

Note: This article provides an excerpt of Geologic Time Scale 2004 (Cambridge University Press, ~500 pp.). The Time Scale Project is a joint undertaking of F.M. Gradstein, J.G. Ogg, A.G. Smith, F.P. Agterberg, W. Bleeker, R.A. Cooper, V. Davydov, P. Gibbard, L.A. Hinnov, M.R. House (†), L.J. Lourens, H-P. Luterbacher, J. McArthur, M.J. Melchin, L.J. Robb, J. Shergold, M. Villeneuve, B.R. Wardlaw, J. Ali, H. Brinkhuis, F.J. Hilgen, J. Hooker, R.J. Howarth, A.H. Knoll, J. Laskar, S. Monechi, J. Powell, K.A. Plumb, I. Raffi, U. Röhl, A. Sanfilippo, B. Schmitz, N.J. Shackleton, G.A. Shields, H. Strauss, J. Van Dam, J. Veizer, Th. van Kolfschoten, and D. Wilson, and is under auspices of the International Commission on Stratigraphy.

international chronostratigraphic scale. In some cases, such as in the Ordovician or Permian periods, traditional European- or Asian-based geological stages have been replaced with new subdivisions that allow global correlation.

(2) New or enhanced methods of extracting linear time from the rock record have enabled high-precision age assignments. Numerous high-resolution radiometric dates have been generated that has led to improved age assignments of key geologic stage boundaries. The use of global geochemical variations, Milankovitch climate cycles, and magnetic reversals have become important calibration tools.

(3) Statistical techniques of interpolating ages and associated uncertainties to stratigraphic events have evolved to meet the challenge of more accurate age dates and more precise zonal assignments. Fossil event databases with multiple stratigraphic sections through the globe can be integrated into high-resolution composite standards for internal scaling of geologic stages.

The compilation of GTS2004 involved a large number of specialists, listed above, including contributions by past and present chairs of different subcommissions of ICS, geochemists working with radiogenic and stable isotopes, stratigraphers using diverse tools from traditional fossils to astronomical cycles to database programming, and geomathematicians.

The methods used to construct Geologic Time Scale 2004 (GTS2004) integrate different techniques depending on the quality of data available within different intervals (Figure 1). The set of chronostratigraphic units (geologic stages, periods) and their computed ages that constitute the main framework for the Geologic Time Scale 2004 are summarized in the International Stratigraphic Chart (Figure 2 and accompanying insert). Uncertainties on ages are expressed at 2-sigma (95% confidence). Table 1 summarizes the status of stratigraphic standardization, compiled by one of us (JGO), for the entire geologic column. Steady progress is made with further standardization of the stratigraphic scale.

The main steps involved in the GTS2004 time scale construction were:

Step 1. Construct an updated global chronostratigraphic scale for the Earth's rock record (Table 1).

Step 2. Identify key linear-age calibration levels for the chronostratigraphic scale using radiometric age dates, and/or apply

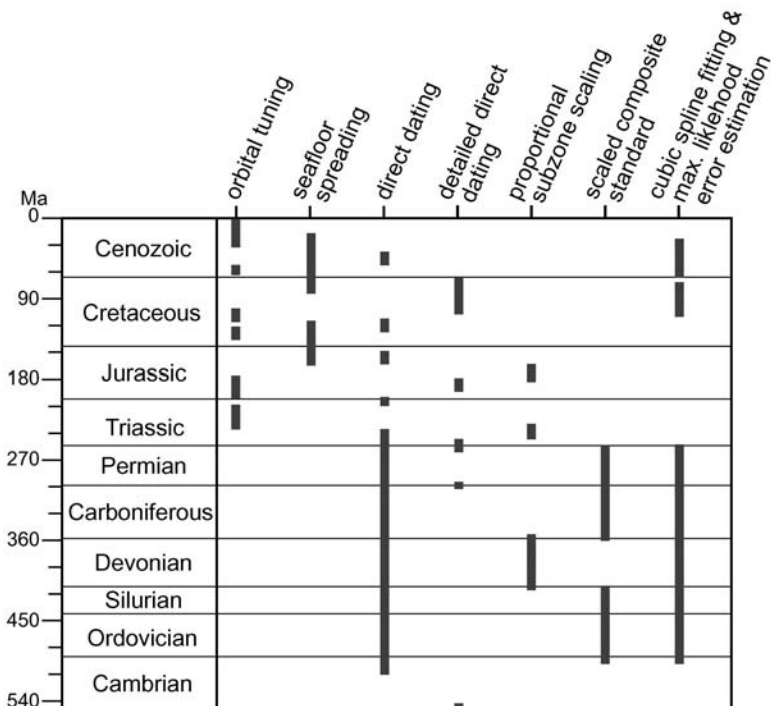


Figure 1 Methods used to construct the Geologic Time Scale 2004 (GTS2004) integrate different techniques depending on the quality of data available within different intervals.

astronomical tuning to cyclic sediment or stable isotope sequences which had biostratigraphic or magnetostratigraphic correlations.

Step 3. Interpolate the combined chronostratigraphic and chronometric scale where direct information is insufficient.

Step 4. Calculate or estimate error bars on the combined chronostratigraphic and chronometric information to obtain a geologic time scale with estimates of uncertainty on boundaries and on unit durations.

Step 5. Peer review the geologic time scale through ICS.

The first step, integrating multiple types of stratigraphic information in order to construct the chronostratigraphic scale, is the most time-consuming. This relative geologic time scale summarizes and synthesizes centuries of detailed geological research. The second step, identifying which radiometric and cycle-stratigraphic studies would be used as the primary constraints for assigning linear ages, is the one that is evolved most rapidly during the past decade. Historically, Phanerozoic time scale building went from an exercise with very few and relatively inaccurate radiometric dates, as used by Holmes (1947, 1960), to one with many dates with greatly varying analytical precision (like GTS89, or to some extent Gradstein et al., 1994). Next came studies on relatively short stratigraphic intervals that selected a few radiometric dates with high internal analytical precision (e.g., Obradovich, 1993; Cande & Kent, 1992, 1995; Cooper, 1999) or measured time relative to present using astronomical cycles (e.g., Shackleton et al., 1999; Hilgen et al., 1995, 2000). This later philosophy is adhered to in this scale.

In addition to selecting radiometric ages based upon their stratigraphic control and analytical precision, we also applied the following criteria or corrections:

(1) Stratigraphically constrained radiometric ages with the U-Pb method on zircons were accepted from the isotope dilution mass spectrometry (TIMS) method, but generally not from the high-resolution ion microprobe (HR-SIMS, also known as "SHRIMP") that uses the Sri Lanka (SL)13 standard. An exception is the Carboniferous Period, where there is a dearth of TIMS dates, and more uncertainty.

(2) ^{40}Ar - ^{39}Ar radiometric ages were re-computed to be in accord with the revised ages for laboratory monitor standards: 523.1 \pm 4.6 Ma for MMhb-1 (Montana hornblende), 28.34 \pm 0.28 Ma for TCR (Taylor Creek sanidine) and 28.02 \pm 0.28 Ma for FCT (Fish Canyon sanidine). Systematic ("external") errors and uncertainties in decay constants are partially incorporated. No glauconite dates are used.

The bases of the Paleozoic, Mesozoic and Cenozoic eras are bracketed by analytically precise ages at their GSSP (Global Standard Section and Point) or primary correlation markers — 542 \pm 1.0 Ma, 251.0 \pm 0.4 Ma, and 65.5 \pm 0.3 Ma — and there are direct age-dates on base-Carboniferous, base-Permian, base-Jurassic, and base-Oligocene; but most other period or stage boundaries prior to the Neogene lack direct age control. Therefore, the third step, interpolation, plays a key role for most of GTS2004. A set of detailed and high-resolution interpolation processes incorporated several techniques, depending upon the available information:

(1) A composite standard of graptolite zones spanning the uppermost Cambrian, Ordovician and Silurian interval was derived from 200+ sections in oceanic and slope environment basins using the constrained optimization method. With zone thickness taken as directly proportional to zone duration, the detailed composite sequence was scaled using selected, high precision zircon and sanidine age dates. For the Carboniferous through Permian a composite standard of conodont, fusulinid, and ammonoids events from many classical sections was calibrated to a combination of U-Pb and ^{40}Ar - ^{39}Ar dates with assigned external error estimates. A composite standard of conodont zones was used for Early Triassic. This procedure directly scaled all stage boundaries and biostratigraphic horizons.



INTERNATIONAL STRATIGRAPHIC CHART

International Commission on Stratigraphy



Eonothem	Era	System	Period	Series	Stage	Age Ma	GSSP		
Phanerozoic	Mesozoic	Cretaceous	Upper	Lower	Albian	112.0 ±1.0	🔑		
					Aptian	125.0 ±1.0			
Barremian	130.0 ±1.5								
Hauterivian	136.4 ±2.0								
Valanginian	140.2 ±3.0								
Berriasian	145.5 ±4.0								
Paleogene	Upper	Paleocene			Lower	Cenomanian		99.6 ±0.9	🔑
						Turonian		93.5 ±0.8	
						Coniacian		89.3 ±1.0	
						Santonian		85.8 ±0.7	
			Campanian	83.5 ±0.7					
			Maastrichtian	70.6 ±0.6					
			Danian	65.5 ±0.3					
			Thanetian	58.7 ±0.2					
			Ypresian	48.6 ±0.2					
			Lutetian	40.4 ±0.2					
Neogene	Upper	Pliocene	Lower	Zanclean	3.600	🔑			
				Piacenzian	2.588				
				Gelasian	1.806				
				Miocene	🔑				
				Serravallian			13.665		
				Langhian			15.97		
				Burdigalian			20.43		
				Aquitanian			23.03		
				Chattian			28.4 ±0.1		
				Cenozoic	Upper		Oligocene	Lower	Rupelian
Priabonian	37.2 ±0.1								
Bartonian	40.4 ±0.2								
Ypresian	55.8 ±0.2								
Thanetian	58.7 ±0.2								
Selandian	61.7 ±0.2								
Danian	65.5 ±0.3								
Maastrichtian	70.6 ±0.6								
Campanian	83.5 ±0.7								
Santonian	85.8 ±0.7								

This chart is copyright protected; no reproduction of any parts may take place without written permission by the International Commission on Stratigraphy.

Eonothem	Era	System	Period	Series	Stage	Age Ma	GSSP
Phanerozoic	Mesozoic	Triassic	Upper	Lower	Rhaetian	199.6 ±0.6	🔑
					Norian	203.6 ±1.5	
Phanerozoic	Mesozoic	Triassic	Upper	Lower	Carnian	216.5 ±2.0	🔑
					Ladinian	228.0 ±2.0	
Phanerozoic	Mesozoic	Triassic	Upper	Lower	Anisian	237.0 ±2.0	🔑
					Olenekian	245.0 ±1.5	
Phanerozoic	Mesozoic	Triassic	Upper	Lower	Induan	249.7 ±0.7	🔑
					Changhsingian	251.0 ±0.4	
Phanerozoic	Mesozoic	Triassic	Upper	Lower	Wuchiapingian	253.8 ±0.7	🔑
					Wuchiapingian	260.4 ±0.7	
Phanerozoic	Mesozoic	Triassic	Upper	Lower	Capitanian	265.8 ±0.7	🔑
					Wordian	268.0 ±0.7	
Phanerozoic	Mesozoic	Triassic	Upper	Lower	Roadian	270.6 ±0.7	🔑
					Kungurian	275.6 ±0.7	
Phanerozoic	Mesozoic	Triassic	Upper	Lower	Artinskian	284.4 ±0.7	🔑
					Sakmarian	294.6 ±0.8	
Phanerozoic	Mesozoic	Triassic	Upper	Lower	Asselian	299.0 ±0.8	🔑
					Gzhelcian	303.9 ±0.9	
Phanerozoic	Mesozoic	Triassic	Upper	Lower	Kasimovian	305.5 ±1.0	🔑
					Moscovian	311.7 ±1.1	
Phanerozoic	Mesozoic	Triassic	Upper	Lower	Bashkirian	318.1 ±1.3	🔑
					Serpukhovian	326.4 ±1.6	
Phanerozoic	Mesozoic	Triassic	Upper	Lower	Viséan	345.3 ±2.1	🔑
					Tournaisian	359.2 ±2.5	

Eonothem	Era	System	Period	Series	Stage	Age Ma	GSSP
Phanerozoic	Paleozoic	Cambrian	Upper	Lower	Palibian	501.0 ±2.0	🔑
					Furongian	513.0 ±2.0	
Phanerozoic	Paleozoic	Cambrian	Upper	Lower	Ordovician	488.3 ±1.7	🔑
					Dartmouthian	460.9 ±1.6	
Phanerozoic	Paleozoic	Cambrian	Upper	Lower	Hirnantian	443.7 ±1.5	🔑
					Rhuddanian	436.0 ±1.9	
Phanerozoic	Paleozoic	Cambrian	Upper	Lower	Aeronian	439.0 ±1.8	🔑
					Telychian	428.2 ±2.3	
Phanerozoic	Paleozoic	Cambrian	Upper	Lower	Sheinwoodian	426.2 ±2.4	🔑
					Homerian	422.9 ±2.5	
Phanerozoic	Paleozoic	Cambrian	Upper	Lower	Wenlock	418.7 ±2.7	🔑
					Ludfordian	411.2 ±2.8	
Phanerozoic	Paleozoic	Cambrian	Upper	Lower	Priddian	416.0 ±2.8	🔑
					Lochkovian	407.0 ±2.8	
Phanerozoic	Paleozoic	Cambrian	Upper	Lower	Pragian	407.0 ±2.8	🔑
					Emsian	397.5 ±2.7	
Phanerozoic	Paleozoic	Cambrian	Upper	Lower	Eifelian	391.8 ±2.7	🔑
					Givetian	385.3 ±2.6	
Phanerozoic	Paleozoic	Cambrian	Upper	Lower	Frasnian	374.5 ±2.6	🔑
					Famennian	359.2 ±2.5	

Eonothem	Era	System	Period	Age Ma	GSSP
Phanerozoic	Paleozoic	Archean	Lower limit is not defined	3600	🔑
				3320	🔑
Phanerozoic	Paleozoic	Archean	Lower limit is not defined	2800	🔑
				2500	🔑
Phanerozoic	Paleozoic	Archean	Lower limit is not defined	2300	🔑
				2050	🔑
Phanerozoic	Paleozoic	Archean	Lower limit is not defined	1800	🔑
				1600	🔑
Phanerozoic	Paleozoic	Archean	Lower limit is not defined	1400	🔑
				1200	🔑
Phanerozoic	Paleozoic	Archean	Lower limit is not defined	1000	🔑
				850	🔑
Phanerozoic	Paleozoic	Archean	Lower limit is not defined	630	🔑
				542	🔑

Subdivisions of the global geologic record are formally defined by their lower boundary. Each unit of the Phanerozoic interval (~542 Ma to Present) and the base of the Ediacaran is defined by a Global Standard Section and Point (GSSP) at its base, whereas the Precambrian interval is formally subdivided by absolute age, Global Standard Stratigraphic Age (GSSA).

This chart gives an overview of the international chronostratigraphic units, their rank, their names and formal status. These units are approved by the International Commission on Stratigraphy (ICS) and ratified by the International Union of Geological Sciences (IUGS).

The Guidelines of the ICS (Remane et al., 1996, Episodes, 19: 77-81) regulate the selection and

Copyright © 2004 International Commission on Stratigraphy

Figure 2 The International Stratigraphical Chart summarizes the set of chronostratigraphic units (geologic stages, periods) and their computed ages, which are the main framework for Geologic Time Scale 2004. Uncertainties on ages expressed at 2-sigma (95% confidence).

Table 1 Status of defining lower boundaries of geologic stages with GSSPs (as of May, 2004). Updates of this compilation can be obtained from the website (www.stratigraphy.org) of the International Commission on Stratigraphy (ICS) under IUGS.

EON, Era, System, Series, Stage	Age (Ma) GTS2004	Est. \pm myr	Derivation of Age	Principal correlative events	GSSP and location	Status	Publication
PHANEROZOIC							
Cenozoic Era							
Neogene System							
Holocene Series							
base Holocene	11.5 ka	0.00	Carbon-14 dating calibration	exactly 10,000 Carbon-14 years (= 11.5 ka calendar years BP) at the end of the Younger Dryas cold spell		Informal working definition	
Pleistocene Series							
base Upper Pleistocene subseries	0.126	0.00	Astronomical cycles in sediments	base of the Eemian interglacial stage (= base of marine isotope stage 5e) before final glacial episode of Pleistocene	Potentially, within sediment core under the Netherlands (Eemian type area)	Informal working definition	
base Middle Pleistocene subseries	0.781	0.00	Astronomical cycles in sediments	Brunhes-Matuyama magnetic reversal		Informal working definition	
base Pleistocene Series	1.806	0.00	Astronomical cycles in sediments	Just above top of magnetic polarity chronozone C2n (Olduvai) and the extinction level of calcareous nannofossil <i>Discoaster brouweri</i> (base Zone CN13). Above are lowest occurrence of calcareous nannofossil medium <i>Gephyrocapsa</i> spp. and extinction level of planktonic foraminifer <i>Globigerinoides extremus</i> .	Top of sapropel layer 'e', Vrica section, Calabria, Italy	Ratified 1985	<i>Episodes</i> 8 (2), p.116-120, 1985
Pliocene Series							
base Gelasian Stage	2.588	0.00	Astronomical cycles in sediments	Isotopic stage 103, base of magnetic polarity chronozone C2r (Matuyama). Above are extinction levels of calcareous nannofossil <i>Discoaster pentaradiatus</i> and <i>D. surculus</i> (base Zone CN12c).	Midpoint of sapropelic Nicola Bed ("A5"), Monte San Nicola, Gela, Sicily, Italy	Ratified 1996	<i>Episodes</i> 21 (2), p.82-87, 1998
base Piacenzian Stage	3.600	0.00	Astronomical cycles in sediments	Base of magnetic polarity chronozone C2An (Gauss); extinction levels of planktonic foraminifers <i>Globorotalia margaritae</i> (base Zone PL3) and <i>Pulleniatina primalis</i> .	Base of beige layer of carbonate cycle 77, Punta Piccola, Sicily, Italy	Ratified 1997	<i>Episodes</i> 21 (2), p.88-93, 1998
base Zanclean Stage, base Pliocene Series	5.332	0.00	Astronomical cycles in sediments	Top of magnetic polarity chronozone C3r, ~100 kyr before Thvera normal-polarity subchronozone (C3n.4n). Calcareous nannofossils – near extinction level of <i>Triquetrorhabdulus rugosus</i> (base Zone CN10b) and the lowest occurrence of <i>Ceratolithus acutus</i> .	Base of Trubi Fm (base of carbonate cycle 1), Eraclea Minoa, Sicily, Italy	Ratified 2000	<i>Episodes</i> 23 (3), p.179-187, 2000
Miocene Series							
base Messinian Stage	7.246	0.00	Astronomical cycles in sediments	Astrochronology age of 7.246 Ma; middle of magnetic polarity chronozone C3Br.1r; lowest regular occurrence of the <i>Globorotalia conomiozea</i> planktonic foraminifer group.	Base of red layer of carbonate cycle 15, Oued Akrech, Rabat, Morocco	Ratified 2000	<i>Episodes</i> 23 (3), p.172-178, 2000
base Tortonian Stage	11.608	0.00	Astronomical cycles in sediments	Last Common Occurrences of the calcareous nannofossil <i>Discoaster kugleri</i> and the planktonic foraminifer <i>Globigerinoides subquadratus</i> . Associated with the short normal-polarity subchron C5r.2n.	Midpoint of sapropel 76, Monte dei Corvi beach section, Ancona, Italy	Ratified 2003	<i>Episodes</i> article in preparation
base Serravillian Stage	13.65	0.00	Astronomical cycles in sediments	Near lowest occurrence of nannofossil <i>Sphenolithus heteromorphus</i> , and within magnetic polarity chronozone C5ABr.		GSSP anticipated in 2004	
base Langhian Stage	15.97	0.0	Calibrated magnetic anomaly scale	Near first occurrence of planktonic foraminifer <i>Praeorbulina glomerosa</i> and top of magnetic polarity chronozone C5Cn.1n		GSSP anticipated in 2004	
base Burdigalian Stage	20.43	0.0	Calibrated magnetic anomaly scale	Near lowest occurrence of planktonic foraminifer <i>Globigerinoides altiapertura</i> or near top of magnetic polarity chronozone C6An		<i>Guide event is undecided</i>	
base Aquitanian Stage, base Miocene Series, base Neogene System	23.03	0.0	Astronomical cycles in sediments	Base of magnetic polarity chronozone C6Cn.2n; lowest occurrence of planktonic foraminifer <i>Paragloborotalia kugleri</i> ; near extinction of calcareous nannofossil <i>Reticulofenestra bisecta</i> (base Zone NN1).	35 m from top of Lemme-Carrosio section, Carrosio village, north of Genoa, Italy	Ratified 1996	<i>Episodes</i> 20 (1), p.23-28, 1997

(Continued)

EON, Era, System, Series, Stage	Age (Ma) GTS2004	Est. ± myr	Derivation of Age	Principal correlative events	GSSP and location	Status	Publication
Paleogene System							
Oligocene Series							
base Chattian Stage	28.4	0.1	Calibrated magnetic anomaly scale relative to base-Miocene and C24n. Arbitrary 100 kyr uncertainty assigned.	Planktonic foraminifer, extinction of <i>Chiloguembelina</i> (base Zone P21b)	Probably in Umbria-Marche region of Italy	GSSP anticipated in 2004	
base Rupelian Stage, base Oligocene Series	33.9	0.1	Calibrated magnetic anomaly scale relative to base-Miocene and C24n.	Planktonic foraminifer, extinction of <i>Hantkenina</i>	Base of marl bed at 19m above base of Massignano quarry, Ancona, Italy	Ratified 1992	<i>Episodes</i> 16 (3), p.379-382, 1993
Eocene Series							
base Priabonian Stage	37.2	0.1	Calibrated magnetic anomaly scale relative to base-Miocene and C24n.	Near lowest occurrence of calcareous nannofossil <i>Chiasmolithus oamaruensis</i> (base Zone NP18)	Probably in Umbria-Marche region of Italy		
base Bartonian Stage	40.4	0.2	Calibrated magnetic anomaly scale relative to base-Miocene and C24n.	Near extinction of calcareous nannofossil <i>Reticulofenestra reticulata</i>			
base Lutetian Stage	48.6	0.2	Calibrated magnetic anomaly scale relative to base-Miocene and C24n.	Planktonic foraminifer, lowest occurrence of <i>Hantkenina</i>	Leading candidate is Fortuna section, Murcia province, Betic Cordilleras, Spain	GSSP anticipated in 2004	
base Ypresian Stage, base Eocene Series	55.8	0.2	Astronomical cycles in sediments scaled from base-Paleocene	Base of negative carbon-isotope excursion	Dababiya section near Luxor, Egypt	Ratified 2003	<i>Micropaleontology</i> v.49 (Suppl. 1), 2003. <i>Episodes</i> article in preparation
Paleocene Series							
base Thanetian Stage	58.7	0.2	Astronomical cycles in sediments scaled from base Paleocene, using base of magnetic polarity chronozone C26n. Arbitrary 0.1 (2 precession cycles, plus the base-Paleogene radiometric) uncertainty assigned to all estimates.	Magnetic polarity chronozone, base of C26n, is a temporary assignment	Leading candidate is Zumaya section, northern Spain	<i>Guide event is undecided</i>	
base Selandian Stage	61.7	0.2	Astronomical cycles in sediments scaled from base Paleocene, using magnetic polarity chronozone placement of C27n.9	Boundary task group is considering a higher level -- base of calcareous nannofossil zone NP5 -- which would be ~1 myr younger.	Leading candidate is Zumaya section, northern Spain	<i>Guide event is undecided</i>	
base Danian Stage, base Paleogene System, base Cenozoic	65.5	0.3	Ar-Ar and U-Pb age agreement	Iridium geochemical anomaly. Associated with a major extinction horizon (foraminifers, calcareous nannofossils, dinosaurs, etc.);	Base of boundary clay, El Kef, Tunisia (<i>but deterioration may require assigning a replacement section</i>)	Ratified 1991	
Mesozoic Era							
Cretaceous System							
Upper							
base Maastrichtian Stage	70.6	0.6	Estimated placement relative to Ar-Ar calibrated Sr-curve	Mean of 12 biostratigraphic criteria of equal importance. Closely above is lowest occurrence of ammonite <i>Pachydiscus neubergicus</i> . Boreal proxy is lowest occurrence of belemnite <i>Belemnella lanceolata</i> .	115.2 m level in Grande Carrière quarry, Tercis-les-Bains, Landes province, SW France	Ratified 2001	<i>Episodes</i> 24 (4), p.229-238, 2001; Odin (ed.) IUGS Spec. Publ. Series, v.36, Elsevier, 910pp.
base Campanian Stage	83.5	0.7	Spline fit of Ar-Ar ages and ammonite zones.	Crinoid, extinction of <i>Marsupites testudinarius</i>	Leading candidates are in southern England and in Texas		
base Santonian Stage	85.9	0.7	Spline fit of Ar-Ar ages and ammonite zones.	Inoceramid bivalve, lowest occurrence of <i>Cladoceras undulaticatus</i>	Leading candidates are in Spain, England and Texas		
base Coniacian Stage	89.3	1.0	Spline fit of Ar-Ar ages and ammonite zones.	Inoceramid bivalve, lowest occurrence of <i>Cremnoceras rotundatus</i> (<i>sensu</i> Tröger non Fiege)	Base of Bed MK47, Salzgitter-Salder Quarry, SW of Hannover, Lower Saxony, northern Germany	GSSP anticipated in 2004	

(Continued)

EON, Era, System, Series, Stage	Age (Ma) GTS2004	Est. \pm myr	Derivation of Age	Principal correlative events	GSSP and location	Status	Publication
base Turonian Stage	93.6	0.8	Spline fit of Ar-Ar ages and ammonite zones.	Ammonite, lowest occurrence of <i>Watinoceras devonense</i>	Base of Bed 86, Rock Canyon Anticline, east of Pueblo, Colorado, west-central USA	Ratified 2003	<i>Episodes article in preparation</i>
base Cenomanian Stage	99.6	0.9	Spline fit of Ar-Ar ages and ammonite zones, plus monitor standard correction. Then cycle stratigraphy to place foraminifer datum relative to ammonite zonation.	Planktonic foraminifer, lowest occurrence of <i>Rotalipora globotruncanoides</i>	36 m below top of Marnes Bleues Formation, Mont Risou, Rosans, Haute-Alpes, SE France	Ratified 2002	<i>Episodes</i> 27 (1), p.21-32, 2004
Lower							
base Albian Stage	112.0	1.0	Estimated placement relative to bases of Cenomanian and Aptian, with large uncertainty due to lack of GSSP criteria. Ar-Ar age of 114.6 \pm 0.7 Ma from <i>Parahoplites nutfieldensis</i> below.	Calcareous nannofossil, lowest occurrence of <i>Praediscosphaera columnata</i> (= <i>P. cretacea</i> of some earlier studies), is one potential marker.		Guide event is undecided	
base Aptian Stage	125.0	1.0	Base of M0r, as recomputed from Ar-Ar age from MIT guyot	Magnetic polarity chronozone, base of M0r	Leading candidate is Gorgo a Cerbara, Piobbico, Umbria-Marche, central Italy		
base Barremian Stage	130.0	1.5	Pacific spreading model for magnetic anomaly ages (variable rate), using placement at M5n.8.	Ammonite, lowest occurrence of <i>Spitidiscus hugii</i> – <i>Spitidiscus vandeckii</i> group	Leading candidate is Rio Argos near Caravaca, Murcia province, Spain		
base Hauterivian Stage	136.4	2.0	Pacific spreading model for magnetic anomaly ages (variable rate), using placement at base M11n.	Ammonite, lowest occurrence of genus <i>Acanthodiscus</i> (especially <i>A. radiatus</i>)	Leading candidate is La Charce village, Drôme province, southeast France		
base Valanginian Stage	140.2	3.0	Pacific spreading model for magnetic anomaly ages (variable rate), using placement at M14r.3 (base <i>T. pertransiens</i>).	Calpionellid, lowest occurrence of <i>Calpionellites dardeni</i> (base of Calpionellid Zone E); followed by the lowest occurrence of ammonite " <i>Thurmanniceras</i> " <i>pertransiens</i>	Leading candidate is near Montbrun-les-Bains, Drôme province, southeast France		
base Berriasian Stage, base Cretaceous System	145.5	4.0	Pacific spreading model for magnetic anomaly ages (variable rate), assigning to base of <i>Berriasella jacobi</i> zone (M19n.2n.55)	Maybe near lowest occurrence of ammonite <i>Berriasella jacobi</i>		Guide event is undecided	
Jurassic System							
Upper							
base Tithonian Stage	150.8	4.0	Pacific spreading model for magnetic anomaly ages (variable rate), assigning to base M22An	Near base of <i>Hyboniticeras hybonotum</i> ammonite zone and lowest occurrence of <i>Gravesia</i> genus, and the base of magnetic polarity chronozone M22An		Guide event is undecided	
base Kimmeridgian Stage	155.7	4.0	Pacific spreading model for magnetic anomaly ages (variable rate), assigning to base M26r.2 (Boreal ammonite definition)	Ammonite, near base of <i>Pictonia baylei</i> ammonite zone of Boreal realm	Leading candidates are In Scotland, SE France and Poland	GSSP anticipated in 2004	
base Oxfordian Stage	161.2	4.0	Pacific spreading model for magnetic anomaly ages (variable rate), assigning to base M36An	Ammonite, <i>Brightia thuouensis</i> Horizon at base of the <i>Cardioceras scaburgense</i> Subzone (<i>Quenstedtoceras mariae</i> Zone)	Leading candidates are in SE France and southern England	GSSP anticipated in 2004	
Middle							
base Callovian Stage	164.7	4.0	Equal subzones scale Bajo-Bath-Callov	Ammonite, lowest occurrence of the genus <i>Keplerites</i> (<i>Kosmoceratidae</i>) (defines base of <i>Macrocephalites herveyi</i> Zone in sub-Boreal province of Great Britain to southwest Germany)	Leading candidate is Pfeffingen, Swabian Alb, SW Germany	GSSP anticipated in 2004	
base Bathonian Stage	167.7	3.5	Equal subzones scale Bajo-Bath-Callov	Ammonite, lowest occurrence of <i>Parkinsonia</i> (<i>G.</i>) <i>convergens</i> (defines base of <i>Zigzagiceras zigzag</i> Zone)			

(Continued)

EON, Era, System, Series, Stage	Age (Ma) GTS2004	Est. \pm myr	Derivation of Age	Principal correlative events	GSSP and location	Status	Publication
base Bajocian Stage	171.6	3.0	Equal subzones scale Bajo-Bath-Callov	Ammonite, lowest occurrence of the genus <i>Hyperlioceras</i> (defines base of the <i>Hyperlioceras discites</i> Zone)	Base of Bed AB11, 77.8 m above base of Murtinheira section, Cabo Mondego, western Portugal	Ratified 1996	<i>Episodes</i> 20 (1), p.16-22, 1997
base Aalenian Stage	175.6	2.0	Duration of Aalenian-Toarcian from cycle stratigraphy	Ammonite, lowest occurrence of <i>Leioceras</i> genus	base of Bed FZ107, Fuentelsalz, central Spain	Ratified 2000	<i>Episodes</i> 24 (3), p.166-175, 2001
Lower							
base Toarcian Stage	183.0	1.5	Duration of Aalenian-Toarcian from cycle stratigraphy	Ammonite, near lowest occurrence of a diversified <i>Eodactylites</i> ammonite fauna; correlates with the NW European <i>Paltus</i> horizon.		<i>Guide event is undecided</i>	
base Pliensbachian Stage	189.6	1.5	Cycle-scaled linear Sr trend	Ammonite, lowest occurrences of <i>Bifericeras donovani</i> and of genera <i>Apoderoceras</i> and <i>Gleviceras</i> .	Wine Haven section, Robin Hood's Bay, Yorkshire, England, UK	GSSP anticipated in 2003	
base Sinemurian Stage	196.5	1.0	Cycle-scaled linear Sr trend	Ammonite, lowest occurrence of arietitid genera <i>Vermiceras</i> and <i>Metophioceras</i>	0.9 m above base of Bed 145, East Quantoxhead, Watchet, West Somerset, SW England, UK	Ratified 2000	<i>Episodes</i> 25 (1), p.22-26, 2002
base Hettangian Stage, base Jurassic System	199.6	0.6	U-Pb age just below proposed GSSP for base-Jurassic	Near lowest occurrence of smooth <i>Psiloceras planorbis</i> ammonite group		<i>Guide event is undecided</i>	
Triassic System							
Upper							
base Rhaetian Stage	203.3	1.5	Magnetostratigraphic correlation to cycle-scaled Newark magnetic polarity pattern	Near lowest occurrence of ammonite <i>Cochlocera</i> , conodonts <i>Misikella</i> spp. and <i>Epigondolella mosheri</i> , and radiolarian <i>Proparvicingula moniliformis</i> .	Key sections in Austria, British Columbia (Canada), and Turkey	<i>Guide event is undecided</i>	
base Norian Stage	216.5	2.0	Magnetostratigraphic correlation to cycle-scaled Newark magnetic polarity pattern	Base of <i>Klamathites macrolobatus</i> or <i>Stikinoceras kerri</i> ammonoid zones and the <i>Metapolygnathus communisti</i> or <i>M. primitius</i> conodont zones.	Leading candidates are in British Columbia (Canada), Sicily (Italy), and possibly Slovakia, Turkey (Antalya Taurus) and Oman.	<i>Guide event is undecided</i>	
base Carnian Stage	228.0	2.0	Magnetostratigraphic correlation to cycle-scaled Newark magnetic polarity pattern	Near first occurrence of the ammonoids <i>Daxatina</i> or <i>Trachyceras</i> , and of the conodont <i>Metapolygnathus polygnathiformis</i>	Candidate section at Prati di Stuores, Dolomites, northern Italy. Important reference sections in Spiti (India) and New Pass, Nevada (USA).	<i>Guide event is undecided</i>	
Middle							
base Ladinian Stage	237.0	2.0	U-Pb array by Mundil et al. on levels near <i>Nevadites</i> (= <i>Secedensis</i>) ammonite zone in Dolomites, plus placement relative to magnetostratigraphy correlations to cycle-scaled Newark magnetic polarity pattern	Alternate levels are near base of <i>Reitzi</i> , <i>Secedensis</i> , or <i>Curionii</i> ammonite zone; near first occurrence of the conodont genus <i>Budurovignathus</i> .	Leading candidates are Bagolino (Italy) and Felsoos (Hungary). Important reference sections in the Humboldt Range, Nevada (USA).	<i>Guide event is undecided</i>	
base Anisian Stage	245.0	1.5	Proportional subzonal scaling	Ammonite, near lowest occurrences of genera <i>Japonites</i> , <i>Paradanubites</i> , and <i>Paracrochordiceras</i> ; and of the conodont <i>Chiosella timorensis</i>	Candidate section probable at Desli Cair, Dobrogea, Romania; significant sections in Guizhou Province (China).	GSSP anticipated in 2004	
Lower							
base Olenekian Stage	249.7	0.7	Composite standard from conodonts scaled to base-Anisian and base-Triassic	Near lowest occurrence of <i>Hedenstroemia</i> or <i>Meekoceras gracilitatis</i> ammonites, and of the conodont <i>Neospathodus waageni</i> .	Candidate sections in Siberia (Russia) and probably Chaohu, Anhui Province, China. Important sections also in Spiti.	<i>Guide event is undecided</i>	
base Induan Stage, base Triassic System, base Mesozoic	251.0	0.4	U-Pb ages bracket GSSP (Bowring et al., 1998)	Conodont, lowest occurrence of <i>Hindeodus parvus</i> ; termination of major negative carbon-isotope excursion. About 1 myr after peak of Late Permian extinctions.	Base of Bed 27c, Meishan, Zhejiang, China	Ratified 2001	<i>Episodes</i> 24 (2), p.102-114, 2001

(Continued)

EON, Era, System, Series, Stage	Age (Ma) GTS2004	Est. \pm myr	Derivation of Age	Principal correlative events	GSSP and location	Status	Publication	
Paleozoic Era								
Permian System			Permian-Carboniferous time scale is derived from calibrating a master composite section to selected radiometric ages					
Lopingian Series								
base Changhsingian Stage	253.8	0.7		"	Conodont, near lowest occurrence of conodont <i>Clarkina wangi</i>	Leading candidates are in China		
base Wuchiapingian Stage	260.4	0.7		"	Conodont, near lowest occurrence of conodont <i>Clarkina postbitteri</i>	Base of Bed 6K/115 in Penglaitan section, S. bank of Hongshui River, 20 km ESE of Laibin country town, Guangxi, South China	Ratified 2004	
Guadalupian Series								
base Capitanian Stage	265.8	0.7		"	Conodont, lowest occurrence of <i>Jinogondolella postserrata</i>	4.5 m above base of Pinery Limestone Member, Nipple Hill, SE Guadalupe Mountains, Texas, USA	Ratified 2001	<i>Episodes</i> article in preparation
base Wordian Stage	268.0	0.7		"	Conodont, lowest occurrence of <i>Jinogondolella aserrata</i>	7.6 m above base of Getaway Ledge outcrop, Guadalupe Pass, SE Guadalupe Mountains, Texas, USA	Ratified 2001	<i>Episodes</i> article in preparation
base Roadian Stage	270.6	0.7		"	Conodont, lowest occurrence of <i>Jinogondolella nanginkensis</i>	42.7 m above base of Cutoff Formation, Stratotype Canyon, southern Guadalupe Mountains, Texas, USA	Ratified 2001	<i>Episodes</i> article in preparation
Cisuralian Series								
base Kungurian Stage	275.6	0.7		"	Conodont, near lowest occurrence of conodont <i>Neostreptognathus pnevi-N. exculptus</i>	Leading candidates are in southern Ural Mtns.		
base Artinskian Stage	284.4	0.7		"	Conodont, lowest occurrence of conodont <i>Sweetognathus whitei</i>	Leading candidates are in southern Ural Mtns.		
base Sakmarian Stage	294.6	0.8		"	Conodont, near lowest occurrence of conodont <i>Sweetognathus merrelli</i>	Leading candidate is at Kondurovsky, Orenburg Province, Russia.		
base Asselian Stage base Permian System	299.0	0.8		"	Conodont, lowest occurrence of <i>Streptognathodus isolatus</i> within the S "wabaunsensis" conodont chronocline. 6 m higher is lowest fusulinid foraminifer <i>Sphaeroschwagerina vulgaris aktjubensis</i>	27 m above base of Bed 19, Aidaralash Creek, Aktöbe, southern Ural Mountains, northern Kazakhstan	Ratified 1996	<i>Episodes</i> 21 (1), p.11-18, 1998
Carboniferous System								
				Subsystem rank of Mississippian and Pennsylvanian names ratified 2000.				
Pennsylvanian Subsystem				<i>Series classification approved in 2004</i>				
Upper								
base Gzhelian Stage	303.9	0.9	"	Near lowest occurrences of the fusulinids <i>Daixina</i> , <i>Jigulites</i> and <i>Rugosofusulina</i> , or lowest occurrence of conodont <i>Idiognathodus simulator</i> (s.str.). Close to lowest occurrence of ammonoid <i>Shumardites</i>		<i>Guide event is undecided</i>		
base Kasimovian Stage, base Upper Pennsylvanian Series	306.5	1.0	"	Near base of <i>Obsoletes obsoletes</i> and <i>Protriticites pseudomontiparus</i> fusulinid zone, or lowest occurrence of conodont <i>Streptognathodus subexcelsus</i> or of ammonoid <i>Parashumardites</i>		<i>Guide event is undecided</i>		
Middle								
base Moscovian Stage, base Middle Pennsylvanian Series	311.7	1.1	"	Near lowest occurrences of <i>Declinognathodus donetzianus</i> and/or <i>Idiognathoides postsulcatus</i> conodont species, and fusulinid species <i>Aljutovella aljutovica</i> .		<i>Guide event is undecided</i>		
Lower								
base Bashkirian Stage, base Pennsylvanian Subsystem	318.1	1.3	"	Conodont, lowest occurrence of <i>Declinognathodus noduliferus</i> s.l.	82.9 m above top of Battleship Wash Fm., Arrow Canyon, southern Nevada, USA	GSSP ratified 1996.	<i>Episodes</i> 22 (4), p.272-283, 1999	

(Continued)

EON, Era, System, Series, Stage	Age (Ma) GTS2004	Est. \pm myr	Derivation of Age	Principal correlative events	GSSP and location	Status	Publication
Mississippian Subsystem				<i>Series classification approved in 2004</i>			
base Serpukhovian, base Upper Mississippian Series	326.4	1.6	"	Near lowest occurrence of conodont, <i>Lochriea crusiformis</i> .		<i>Guide event is undecided</i>	
base Viséan, base Middle Mississippian Series	345.3	2.1	"	Foraminifer, lineage <i>Eoparastaffella simplex</i> morphotype 1/morphotype 2	Leading candidate is Pengchong, south China		
base Tournaisian, base Mississippian Subsystem, base Carboniferous System	359.2	2.5	"	Conodont, above lowest occurrence of <i>Siphonodella sulcata</i>	Base of Bed 89, La Serre, Montagne Noir, Cabrières, southern France	Ratified 1990	<i>Episodes</i> 14 (4), p.331-336, 1991
Devonian System			Devonian time scale is a statistical fit of a composite biostratigraphic zonation (based on Figure 8 of Williams et al., 2000) to selected radiometric ages				
Upper							
base Famennian Stage	374.5	2.6	"	Just above major extinction horizon (Upper Kellwasser Event), including conodonts <i>Ancyrodella</i> and <i>Ozarkodina</i> and goniatites of <i>Gephuroceratidae</i> and <i>Beloceratidae</i>	base of Bed 32a, upper Coumiac quarry, Cessenon, Montagne Noir, southern France	Ratified 1993	<i>Episodes</i> 16 (4), p.433-441, 1993
base Frasnian Stage	385.3	2.6	"	Conodont, lowest occurrence of <i>Ancyrodella rotundiloba</i> (defines base of Lower <i>Polygnathus asymmetricus</i> conodont Zone)	Base of Bed 42a', Col du Puech de la Suque section, St. Nazaire-de-Ladarez, SE Montagne Noir, southern France	Ratified 1986	<i>Episodes</i> 10 (2), p.97-101, 1987
Middle							
base Givetian Stage	391.8	2.7	"	Conodont, lowest occurrence of <i>Polygnathus hemiansatus</i> , near base of goniatite <i>Maenioceras Stufe</i>	Base of Bed 123, Jebel Mech Irdane ridge, Tafilalt, Morocco	Ratified 1994	<i>Episodes</i> 18 (3), p.107-115, 1995
base Eifelian Stage	397.5	2.7	"	Conodont, lowest occurrence of <i>Polygnathus costatus partitus</i> ; major faunal turnover	Base unit WP30, trench at Wetteldorf Richtschnitt, Schönneck-Wetteldorf, Eifel Hills, western Germany	Ratified 1985	<i>Episodes</i> 8 (2), p.104-109, 1985
Lower							
base Emsian Stage	407.0	2.8	"	Conodont, lowest occurrence of <i>Polygnathus kitabicus</i> (= <i>Po. dehiscens</i>)	Base of Bed 9/5, Zinzil'ban Gorge, SE of Samarkand, Uzbekistan	Ratified 1995	<i>Episodes</i> 20 (4), p.235-240, 1997
base Pragian Stage	411.2	2.8	"	Conodont, lowest occurrence of <i>Eognathodus sulcatus</i>	Base of Bed 12, Velká Chuchle quarry, southwest part of Prague city, Czech Republic	Ratified 1989	<i>Episodes</i> 12 (2), p.109-113, 1989
base Lochkovian Stage, base Devonian System	416.0	2.8	base-Devonian from scale in Cooper (this volume), which is 1 myr younger than Tucker et al (1998) estimate.	Graptolite, lowest occurrence of <i>Monograptus uniformis</i>	Within Bed 20, Klonek, Barrandian area, southwest of Prague, Czech Republic	Ratified 1972	Martinsson (ed.), <i>The Silurian-Devonian Boundary</i> , IUGS Series A, no.5, 349 pp., 1977
Silurian System			Silurian and Ordovician time scales are from calibrating a CONOP composite graptolite zonation to selected radiometric ages				Holland and Bassett (eds), <i>A Global Standard for the Silurian System</i> , Nat. Mus. Wales, Geol. Series No.10, Cardiff, 325 pp., 1989
Pridoli Series							
base Pridoli Series (<i>not subdivided in stages</i>)	418.7	2.7	"	Graptolite, lowest occurrence of <i>Monograptus parulimus</i>	Within Bed 96, Pozáry section near Reporje, Barrandian area, Prague, Czech Republic	Ratified 1984	<i>Episodes</i> 8 (2), p.101-103, 1985
Ludlow Series		2.6					
base Ludfordian Stage	421.3	2.6	"	<i>Imprecise</i> . May be near base of <i>Saetograptus leintwardinensis</i> graptolite zone.	Base of lithological unit C, Sunnyhill Quarry, Ludlow, Shropshire, southwest England, UK	Ratified 1980	<i>Lethaia</i> 14, p.168, 1981; <i>Episodes</i> 5 (3), p.21-23, 1982

(Continued)

EON, Era, System, Series, Stage	Age (Ma) GTS2004	Est. ± myr	Derivation of Age	Principal correlative events	GSSP and location	Status	Publication
base Gorstian Stage	422.9	2.5	"	<i>Imprecise.</i> Just below base of local acritarch <i>Leptobrachion longhopense</i> range zone. May be near base of <i>Neodiversograptus nilssoni</i> graptolite zone.	Base of lithological unit F, Pitch Coppice quarry, Ludlow, Shropshire, southwest England, UK	Ratified 1980	Lethaia 14, p.168, 1981; <i>Episodes</i> 5 (3), p.21-23, 1982
Wenlock Series							
base Homerian Stage	426.2	2.4	"	Graptolite, lowest occurrence of <i>Cyrtograptus lundgreni</i> (defines base of <i>C. lundgreni</i> graptolite zone)	Graptolite biozone intersection in stream section in Whitwell Coppice, Homer, Shropshire, southwest England, UK	Ratified 1980	Lethaia 14, p.168, 1981; <i>Episodes</i> 5 (3), p.21-23, 1982
base Sheinwoodian Stage	428.2	2.3	"	<i>Imprecise.</i> Between the base of acritarch biozone 5 and extinction of conodont <i>Pterospathodus amorphognathoides</i> . May be near base of <i>Cyrtograptus centrifugus</i> graptolite zone.	Base of lithological unit G, Hughley Brook, Apedale, Shropshire, southwest England, UK	Ratified 1980	Lethaia 14, p.168, 1981; <i>Episodes</i> 5 (3), p.21-23, 1982
Llandovery Series							
base Telychian Stage	436.1	1.9	"	Brachiopods, just above extinction of <i>Eocoelia intermedia</i> and below lowest succeeding species <i>Eocoelia curtisi</i> . Near base of <i>Monograptus turriculatus</i> graptolite zone.	Locality 162 in transect d, Cefn Cerig road, Llandovery area, south-central Wales, UK	Ratified 1984	<i>Episodes</i> 8 (2), p.101-103, 1985
base Aeronian Stage	439.0	1.8	"	Graptolite, lowest occurrence of <i>Monograptus austerus sequens</i> (defines base of <i>Monograptus triangularis</i> graptolite zone)	Base of locality 72 in transect h, Trefawr forestry road, north of Cwm-coed-Aeron Farm, Llandovery area, south-central Wales, UK	Ratified 1984	<i>Episodes</i> 8 (2), p.101-103, 1985
base Rhuddanian Stage, base Silurian System	443.7	1.5	"	Graptolites, lowest occurrences of <i>Parakidograptus acuminatus</i> and <i>Akidograptus ascensus</i>	1.6 m above base of Birkhill Shale Fm., Dob's Linn, Moffat, Scotland, UK	Ratified 1984	<i>Episodes</i> 8 (2), p.98-100, 1985
Ordovician System							
Upper							
base Hirnantian Stage	445.6	1.5	"	Potentially at base of the <i>Normalograptus extraordinarius-N. ojsuensis</i> graptolite biozone	Candidate section is Wangjiawan, China		
base of sixth stage (<i>not yet named</i>)	455.8	1.6	"	Potentially near first appearance of the graptolite <i>Diplacanthograptus caudatus</i>	Candidate sections at Black Knob Ridge (Oklahoma, USA) and Hartfell Spa (S. Scotland, UK)		
base of fifth stage (<i>not yet named</i>)	460.9	1.6	"	Graptolite, lowest occurrence of <i>Nemagraptus gracilis</i>	1.4 m below phosphorite in E14a outcrop, Fågelsång, Scane, southern Sweden	Ratified 2002	<i>Episodes</i> 23 (2), p.102-109, 2000 (<i>proposal; formal GSSP publication in preparation</i>).
Middle							
base Darriwilian Stage	468.1	1.6	"	Graptolite, lowest occurrence of <i>Undulograptus austrodentatus</i>	Base of Bed AEP184, 22 m below top of Ningkuo Fm., Huangnitang, Changshan, Zhejiang province, southeast China	Ratified 1997	<i>Episodes</i> 20 (3), p.158-166, 1997
base of third stage (<i>not yet named</i>)	471.8	1.6	"	Conodont, potentially lowest occurrence of <i>Protoprioniodus aranda</i> or of <i>Baltoniodus triangularis</i>	Candidate sections at Niquivil (Argentina) and Huanghuachang (China)		
Lower							
base of second stage (<i>not yet named</i>)	478.6	1.7	"	Graptolite, lowest occurrence of <i>Tetragraptus approximatus</i>	Just above E bed, Diabasbrottet quarry, Västergötland, southern Sweden	Ratified 2002	<i>Episodes</i> article in preparation
base of Tremadocian Stage, base Ordovician System	488.3	1.7	"	Conodont, lowest occurrence of <i>Iapetognathus fluctivagus</i> ; just above base of <i>Cordylodus lindstromi</i> conodont Zone. Just below lowest occurrence of planktonic graptolites. Currently dated around 489 Ma.	Within Bed 23 at the 101.8 m level, Green Point, western Newfoundland, Canada	Ratified 2000	<i>Episodes</i> 24 (1), p.19-28, 2001.
Cambrian System							
Upper ("Furongian") Series							
				Potential GSSP correlation levels include <i>Cordylodus proavus</i> , <i>Glyptagnostus reticulatus</i> , <i>Ptychagnostus punctuosus</i> , <i>Acidusus atavus</i> , and <i>Oryctocephalus indicus</i> .			Overview of potential subdivisions in <i>Episodes</i> 23 (3), p.188-195, 2000.

(Continued)

EON, Era, System, Series, Stage	Age (Ma) GTS2004	Est. \pm myr	Derivation of Age	Principal correlative events	GSSP and location	Status	Publication
<i>upper stage(s) in Furongian</i>				<i>Potential GSSP levels in upper Cambrian are based on trilobites and condonts</i>			
base Paibian Stage, base Furongian Series	501.0	2.0	Radiometric ages near primary marker level. Estimated age and uncertainty only.	Trilobite, lowest occurrence of agnostoid <i>Glyptagnostus reticulatus</i> . Coincides with base of large positive carbon-isotope excursion.	369.06 m above base of Huaqiao Fm, Paibi section, NW Hunan province, south China	Ratified 2003	<i>Episodes article in preparation</i>
Middle	513.0	2.0	Radiometric ages near primary marker level. Estimated age and uncertainty only.	<i>Potential GSSP levels in Middle Cambrian are based mainly on trilobites</i>			
Lower				<i>Potential GSSP levels in Lower Cambrian are based on archaeocyatha, small shelly fossils, and to a lesser extent, trilobites</i>			
base Cambrian System, base Paleozoic, base PHANEROZOIC	542.0	1.0	U-Pb age from Oman coinciding with the negative carbon excursion.	Trace fossil, lowest occurrence of <i>Treptichnus (Phycodes) pedum</i> . Near base of negative carbon-isotope excursion.	2.4 m above base of Member 2 of Chapel Island Fm., Fortune Head, Burin Peninsula, southeast Newfoundland, Canada	Ratified 1992	<i>Episodes</i> 17 (1&2), p.3-8, 1994.
PROTEROZOIC				<i>Pre-Cambrian eras and systems below Ediacaran are defined by absolute ages, rather than stratigraphic points.</i>			
Neoproterozoic Era							
base Ediacaran System	630		Age as suggested by Ediacaran Subcomm.; bracketed by radiometric ages of 600 and 635 Ma	Termination of Marinoan (or Varanger) glaciation, and distinctive C-13 change.	Base of the Marinoan cap carbonate (Nuccaleena Formation), immediately above the Elatina diamictite in the Enorama Creek section, Flinders Ranges, South Australia.	"Neoproterozoic III" (ratified 1990 with base defined chronometrically at 650 Ma) was formally replaced by Ediacaran Period and its GSSP in Feb 2004	
Cryogenian System	850		Defined chronometrically	Base = 850 Ma			
Tonian System	1000		Defined chronometrically	Base = 1000 Ma		Ratified 1990	<i>Episodes</i> 14 (2), p.139-140, 1991
Mesoproterozoic Era							
Stenian System	1200		Defined chronometrically	Base = 1200 Ma		Ratified 1990	<i>Episodes</i> 14 (2), p.139-140, 1991
Ectasian System	1400		Defined chronometrically	Base = 1400 Ma		Ratified 1990	<i>Episodes</i> 14 (2), p.139-140, 1991
Calymmian System	1600		Defined chronometrically	Base = 1600 Ma		Ratified 1990	<i>Episodes</i> 14 (2), p.139-140, 1991
Paleoproterozoic Era							
Statherian System	1800		Defined chronometrically	Base = 1800 Ma		Ratified 1990	<i>Episodes</i> 14 (2), p.139-140, 1991
Orosirian System	2050		Defined chronometrically	Base = 2050 Ma		Ratified 1990	<i>Episodes</i> 14 (2), p.139-140, 1991
Rhyacian System	2300		Defined chronometrically	Base = 2300 Ma		Ratified 1990	<i>Episodes</i> 14 (2), p.139-140, 1991
Siderian System	2500		Defined chronometrically	Base = 2500 Ma		Ratified 1990	<i>Episodes</i> 14 (2), p.139-140, 1991
ARCHEAN							
Neoproterozoic Era	2800		Defined chronometrically	Base = 2800 Ma		Ratified 1990	<i>Episodes</i> 14 (2), p.139-140, 1991
Mesoarchean Era	3200		Defined chronometrically	Base = 3200 Ma		Ratified 1990	<i>Episodes</i> 14 (2), p.139-140, 1991
Paleoarchean Era	3600		Defined chronometrically	Base = 3600 Ma		Ratified 1990	<i>Episodes</i> 14 (2), p.139-140, 1991
Eoarchean Era			Base is not defined				

(2) Detailed direct ages for Upper Cretaceous ammonite zones of the Western Interior of the USA were obtained by a cubic spline fit of the zonal events and 25 ^{40}Ar - ^{39}Ar dates. The base-Turonian age is directly bracketed by this ^{40}Ar - ^{39}Ar set, and ages of other stage boundaries and stratigraphic events are estimated using calibrations to this primary scale.

(3) Seafloor spreading interpolations were done on a composite marine magnetic lineation pattern for the Late Jurassic through Early Cretaceous in the Western Pacific and for the late Cretaceous through early Neogene in the South Atlantic Oceans. Ages of biostratigraphic events were assigned according to their calibration to these magnetic polarity time scales.

(4) Astronomical tuning of cyclic sediments was used for Neogene and Upper Triassic, and for portions of the Lower and Middle Jurassic, Lower Cretaceous, and Paleocene. The Neogene astronomical scale is directly tied to the Present; the older astronomical scale provides absolute-duration constraints on polarity chrons, biostratigraphic zones and entire stages.

(5) Proportional scaling relative to component biozones or subzones. In intervals where none of the above information under Items 1 through 4 was available, it was necessary to return to the methodology employed by previous time scales. This procedure was necessary in portions of the Middle Triassic, and Middle Jurassic. Devonian stages were scaled from approximate equal duration of a set of high-resolution subzones of ammonoids and conodonts, fitted to an array of high-precision dates.

The geomathematics employed for data sets (Items 1, 2, 3 and 5) constructed for the Ordovician-Silurian, Devonian, Carboniferous-Permian, Late Cretaceous, and Paleogene intervals involved cubic spline curve fitting to relate the observed ages to their stratigraphic position. During this process, the ages were weighted according to their variances based on the lengths of their error bars. A chi-square test was used for identifying and reducing the weights of relatively few outliers with error bars that are much narrower than could be expected on the basis of most ages in the data set.

Stratigraphic uncertainty was incorporated in the weights assigned to the observed ages during the spline-curve fitting. In the final stage of analysis, Ripley's algorithm for Maximum Likelihood fitting of a Functional Relationship (MLFR) was used for error estimation, resulting in 2-sigma (95% confidence) error bars for the computed chronostratigraphic boundary ages and stage durations. The uncertainties on older stage boundaries generally increase owing to potential systematic errors in the different radiometric methods, rather than to the analytical precision of the laboratory measurements. In this connection, we mention that biostratigraphic error is fossil event and fossil zone dependent, rather than dependent on linear age.

In Mesozoic intervals that were scaled using the seafloor spreading model or proportionally scaled using paleontological subzones, the assigned uncertainties are conservative estimates based on variability observed when applying different assumptions (see discussions in the Triassic, Jurassic and Cretaceous chapters of GTS2004). Ages and durations of Neogene stages derived from orbital tuning are considered to be accurate within a precession cycle (~20 kyr), assuming that all cycles are correctly identified, and that the theoretical astronomical-tuning for progressively older deposits is precise.

Precambrian

From the time of initial accretion and differentiation (ca. 4560 Ma) to the first appearance of abundant hard-bodied fossils (the onset of the Cambrian Period at 542 Ma), the Precambrian spans 88 percent of Earth history. Yet, there is no coherent view of a geological time scale to help describe, analyze, calibrate, and communicate the evolution of planet Earth.

The *status quo* is a geological time scale for the Precambrian that is both incomplete and flawed (e.g., Cloud, 1987; Crook, 1989;

Nisbet, 1991; Bleeker, 2003a), and is defined in terms of arbitrary, strictly chronometric, absolute age boundaries that are divorced from the only primary, objective, record of planetary evolution: the extant rock record.

At a recent conference in Canada on the geological time scale and its calibration (NUNA, 2003), co-sponsored by the International Committee on Stratigraphy (ICS), there was broad consensus on the view that this arbitrary, chronometrically defined, Precambrian time scale fails to convey the richness of the Precambrian rock record and therefore impedes scientific understanding of geological processes by diverting attention away from observable, first-order, stratigraphic boundaries and transitions.

Specific criticisms of the present Precambrian time scale are outlined in the chapter on Precambrian by Bleeker in Gradstein et al. (2004), but one key point deserves elaboration here: the uncertainty in decay constants of ^{238}U and ^{235}U . These uncertainties (e.g., Ludwig, 2000) conspire in such a way that most age dates for the Precambrian (predominantly upper intercept $^{207}\text{Pb}/^{206}\text{Pb}$ zircon ages, particularly prior to 1 Ga) have a non-trivial fundamental "fuzziness" (e.g., about ± 6.5 million years at ca. 2500 Ma). This fundamental uncertainty increases to ± 10 million years at 4000 Ma. Definition of boundaries in terms of arbitrary, round, absolute ages, although superficially appealing, is therefore naïve. Absolute-age correlation of such boundaries between distant sections, on the basis of even our best geochronometer (U-Pb ages on single zircons), can be no better than ± 5 – 10 million years (in terms of linear ages), even if all other sources of uncertainty (e.g., analytical scatter, Pb loss, or cryptic inheritance) are negligible. In principle, this fundamental uncertainty could be reduced by defining boundaries explicitly in terms of $^{207}\text{Pb}/^{206}\text{Pb}$ zircon ages or isotopic ratios, rather than linear age, but this would make any time scale even less transparent. Furthermore, it would not solve the problem of intercalibration between different chronometers.

Clearly, there can only be one conclusion: the Precambrian time scale should be (re)defined in terms of the only objective physical standard we have, the extant rock record. Boundaries should be placed at key events or transitions in the stratigraphic record, to highlight important milestones in the evolution of our planet. This would be analogous to the "golden spike" GSSP approach employed in the Phanerozoic. Various geochronometers (U-Pb; ^{40}Ar - ^{39}Ar ; Re-Os, etc.), each with their own inherent but independent uncertainties, should be employed to calibrate meaningful stratigraphic boundaries in linear time. The ultimate result should be a calibrated "natural" time scale for planet Earth that reflects first-order events and transitions in its complex evolution.

To achieve this 'natural' time scale we propose that the 2004–2008 mandate of the International Subcommittee on the Precambrian under ICS is a comprehensive and internally consistent, as well as practical, "natural" time scale for planet Earth. This 'natural' time scale should be complete with agreed upon "golden spikes" and type sections (i.e., GSSPs) for all Precambrian eon and era boundaries, and, where needed, for those of periods (systems).

Such an international effort would help focus significant attention on key stratigraphic boundaries and type sections, and, in turn, will stimulate multidisciplinary science into the causes for specific boundaries and transitions, the fundamental processes involved, their rates, and their calibration in absolute time.

Building on efforts by the previous Subcommittee on Precambrian Stratigraphy (e.g., Plumb, 1991), such a "naturalizing" of the Precambrian time scale could largely preserve existing nomenclature, in so far as it has gained acceptance in the literature, while formalizing other eon and era names that are in widespread use today, e.g. the Hadean. Thus, by 2008, we would have, for the first time, a complete and natural time scale that reflects and communicates the entire, protracted, and complex evolution of planet Earth.

Figures 3 and 4 highlight the key points of this discussion. Figure 3 shows the formal current subdivision of the Precambrian, annotated with known key events in Earth's evolution. The practical Geon scale from Hofmann (1990, 1991) provides a quick chronometric shorthand notation. The interval highlighted "early Earth" is

an informal designation commonly used for Earth's first giga-year from the time of accretion to ~3.5 Ga. Exponentially decreasing impact intensity (curve on right) is schematic and includes the "late heavy bombardment" episode. Stars indicate Sudbury and Vredefort impact craters with diameters >50 km.

In the proposed "natural" Precambrian time scale, Earth history is divided into six eons, with boundaries defined by what can be con-

sidered first-order "watersheds" in the evolution of our planet (Figure 4). The six eons can be briefly characterized as follows:

- (1) "Accretion & Differentiation" — planet formation, growth and differentiation up to the Moon-forming giant impact event;
- (2) Hadean (Cloud, 1972) — intense bombardment and its consequences, but no preserved supracrustals;

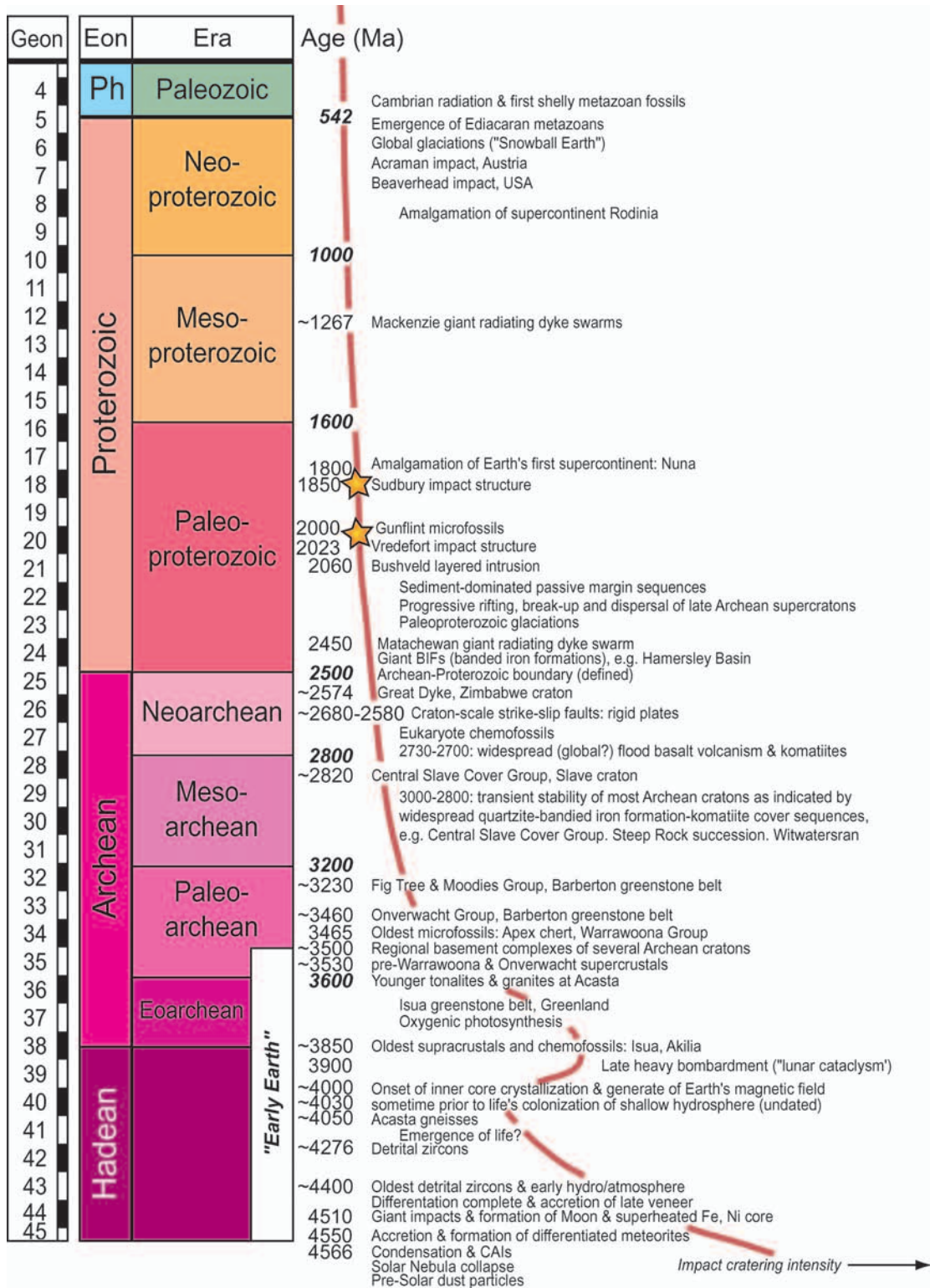


Figure 3 Formal subdivisions of the Precambrian annotated with key events in Earth's evolution. Geon scale from Hofmann (1990, 1991) provides a quick chronometric shorthand notation.

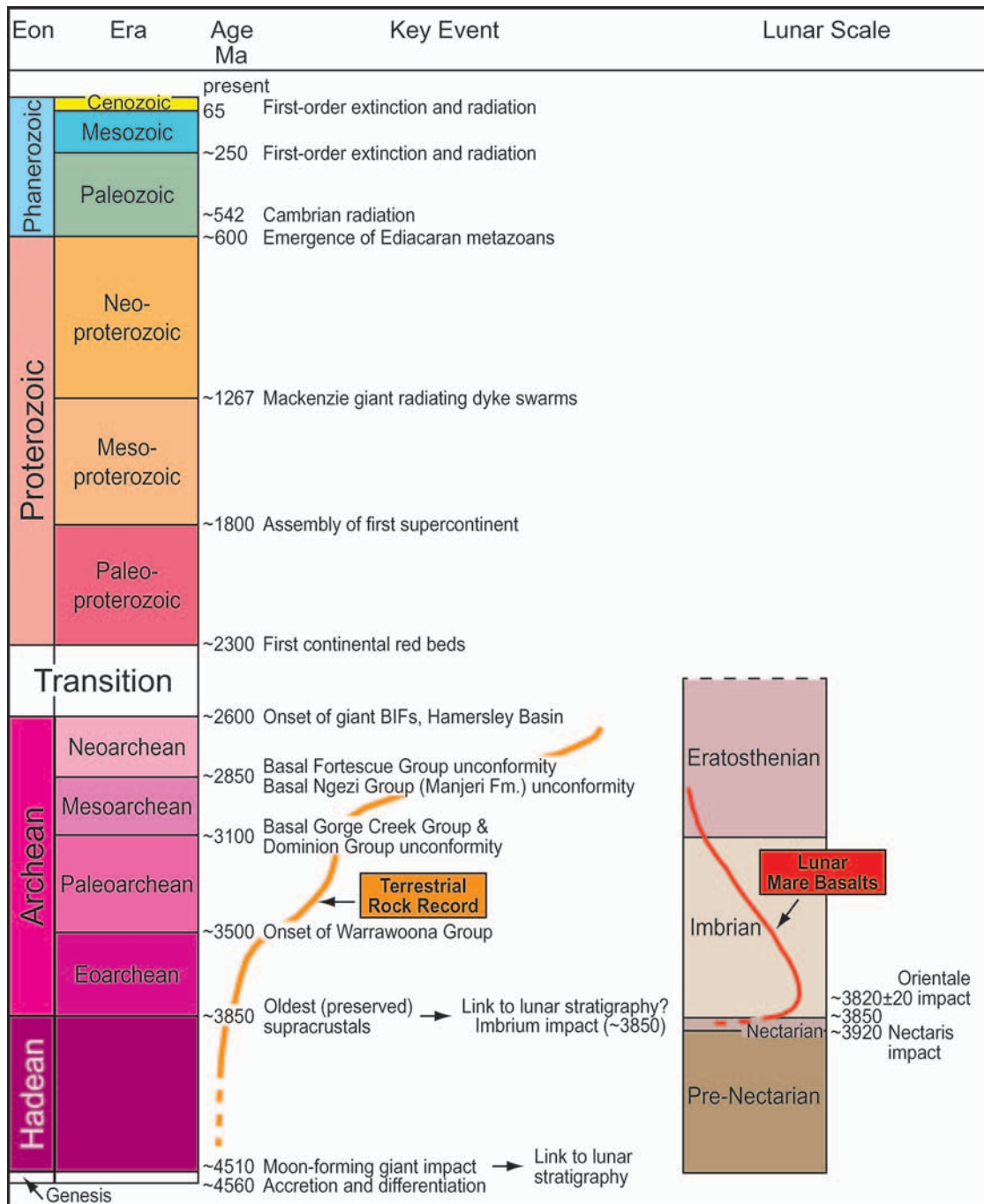


Figure 4 Proposal for a “natural” Precambrian time scale. Earth history is divided into six eons, with boundaries defined by what can be considered first-order key events in the evolution of our planet.

(3) Archean — increasing crustal record from the oldest supracrustals of Isua greenstone belt to the onset of giant iron formation deposition in the Hamersley basin, likely related to increasing oxygenation of the atmosphere;

(4) “Transition” — starting with deposition of giant iron formations up to the first bona fide continental red beds;

(5) Proterozoic — a nearly modern plate-tectonic Earth but without metazoan life, except at its very top; and

(6) The Phanerozoic— characterized by metazoan life forms of increasing complexity and diversity.

Some of the boundaries are currently poorly calibrated in absolute time, whereas the onset of the Archean should “float” with the oldest preserved supracrustal rocks, a distinction currently held by ~3820–3850 Ma rocks of the Isua greenstone belt. Comparison is

shown to the lunar time scale (e.g., Guest and Greeley, 1977; Murray et al., 1981; Spudis, 1999).

Neogene

The most detailed segment of the modern geologic time scale in terms of resolution and accuracy is that for the Neogene, 23 Ma to Recent. The subdivision of the Neogene into its constituent stages is presently well established and internationally accepted for the pre-Pleistocene part (Table 1). New ICS task groups have been organized under the umbrella of the Subcommission on Quaternary Stratigraphy to establish an international Pleistocene subdivision of Lower, Middle and Upper, and to define the Holocene/Pleistocene

boundary. GSSPs have been formalized for the Aquitanian (defining the Paleogene/Neogene boundary), Tortonian and Messinian stages of the Miocene, and for the Zanclean, Piacenzian and Gelasian stages of the Pliocene. In addition, the Pliocene-Pleistocene boundary has been defined.

From the 1970's until 1994, Neogene time scales were constructed using a limited number of radio-isotopic age calibration points in geomagnetic polarity sequences that were primarily derived from a seafloor anomaly profile in the south Atlantic, modified after Heitzler et al. (1968). Biozonations and stage boundaries were subsequently tied to the resulting geomagnetic polarity time scale (GPTS), preferably via magneto-biostratigraphic calibrations

(Berggren et al., 1985). Alternatively, radio-isotopic age determinations from both sides of stage boundaries were used to calculate a best-fit radio-isotopic age estimate for these boundaries in a statistical way (chronogram method of Harland et al., 1982, 1990).

The "standard" method to construct time scales changed drastically with the advent of the astronomical dating method to the prelate Pleistocene. This method relies on the calibration, or tuning, of sedimentary cycles or cyclic variations in climate proxy records to target curves derived from astronomical solutions for the solar-planetary and Earth-Moon systems. Quasi-periodic perturbations in the shape of the Earth's orbit and the tilt of the inclination axis are caused by gravitational interactions of our planet with the Sun, the

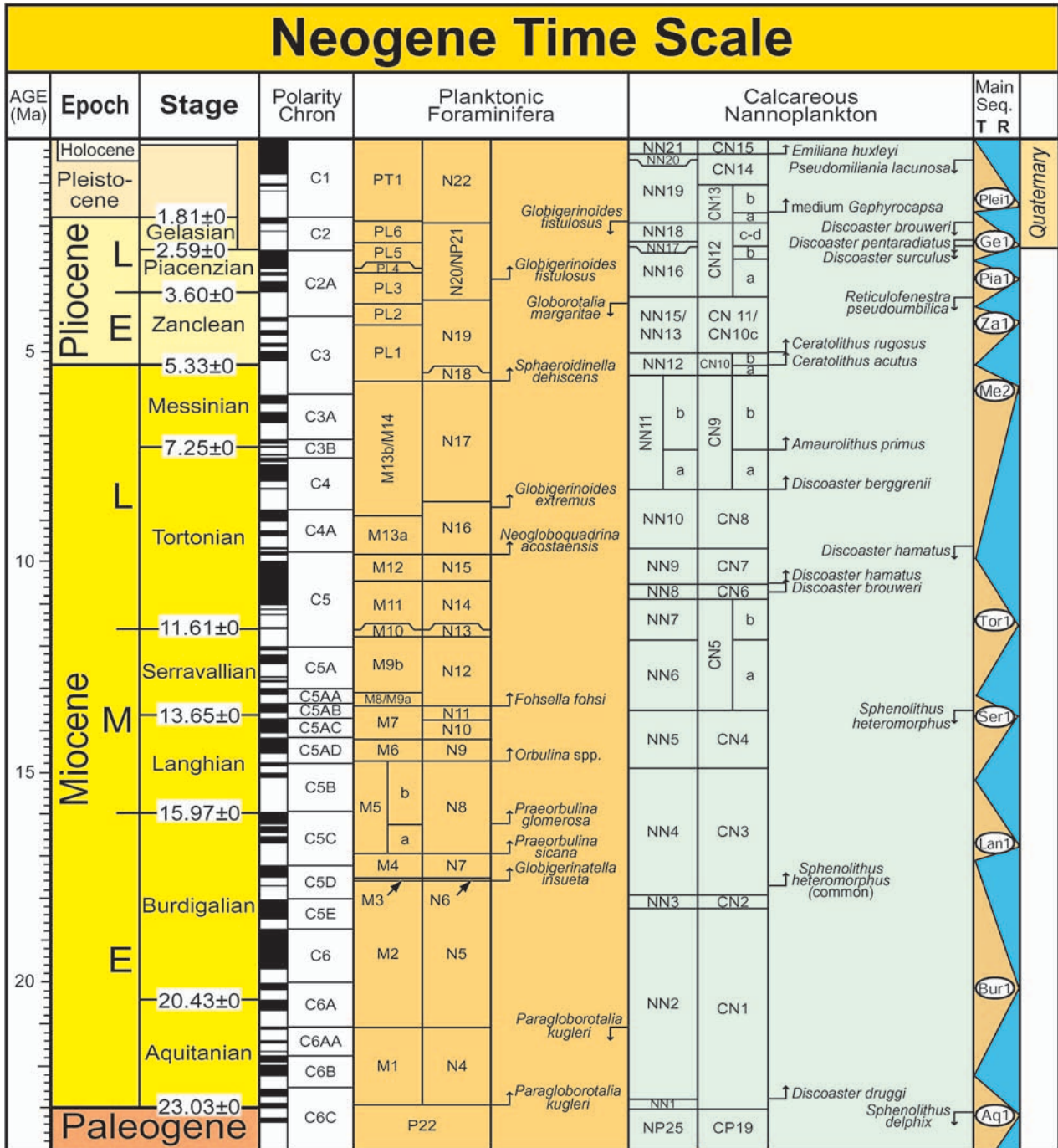


Figure 5a Neogene stratigraphic subdivisions, geomagnetic polarity scale, pelagic zonation and selected datums of planktonic foraminifers and calcareous nannoplankton. Main trends in eustatic sea level are generalized. The "Quaternary", shown schematically on the right-hand side, is traditionally considered to be the interval of oscillating climatic extremes (glacial and interglacial episodes) that was initiated at about 2.6 Ma, therefore encompassing the Holocene and Pleistocene epochs and Gelasian stage of late Pliocene. The Quaternary composite epoch is not a formal unit in the chronostratigraphic hierarchy.

Moon and the other planets of our solar system. These interactions give rise to cyclic changes in the eccentricity of the Earth's orbit, with main periods of 100,000 and 413,000 years, and in the tilt (obliquity) and precession of the Earth's axis with main periods of 41,000, and 21,000 years, respectively (Berger, 1977). These perturbations in the Earth's orbit and rotation axis are climatically important because they affect the global, seasonal and latitudinal distribution of the incoming solar insolation. Orbital forced climate oscillations are recorded in sedimentary archives through changes in sediment properties, fossil communities, chemical and isotopic characteristics. While Earth scientists can read these archives to reconstruct paleoclimate, astronomers have formulated models based on the mechanics of the solar-planetary system and the Earth-Moon system to compute the past variations in precession, obliquity and eccentricity of the Earth's orbit and rotation axis. As a logical next step, sed-

imentary archives can be dated by matching patterns of paleoclimate variability with patterns of varying solar energy input computed from the astronomical model solutions. This astronomical tuning of the sedimentary record results in time scales based on measurable physical parameters that are independent from those underlying radio-isotopic dating and that are tied to the Recent through a direct match with astronomical curves.

Astronomical tuning was first applied in the late Pleistocene in order to build a common high-resolution time scale for the study of orbital induced glacial cyclicality. Initial attempts to extend this time scale back in time were unsuccessful due to lack of resolution or incompleteness of the sedimentary succession. These problems were overcome with the advent of the advanced piston corer (APC) technique in ocean drilling and the drilling of multiple offset holes per site. Combined these innovations were used to construct spliced

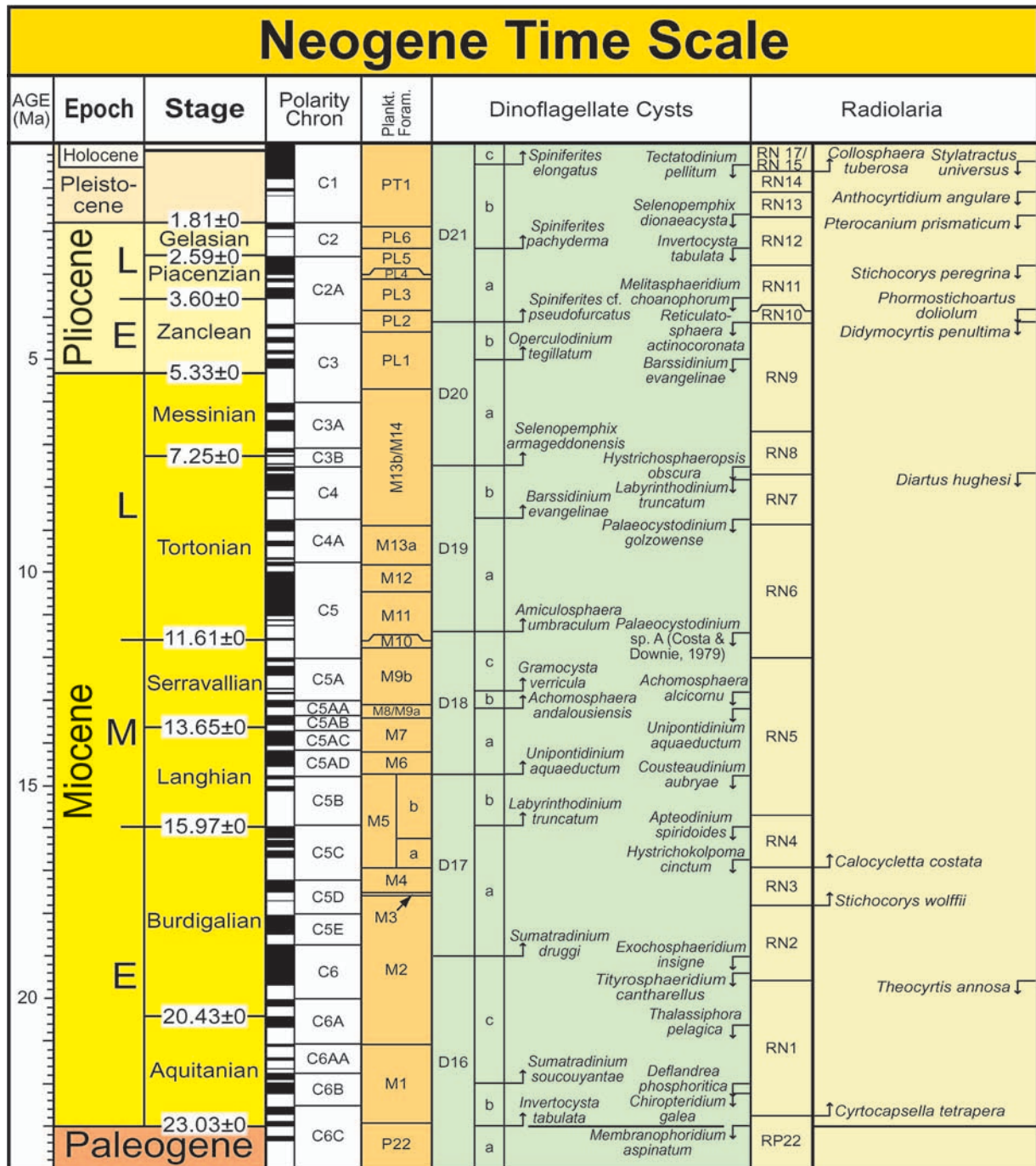


Figure 5b Neogene dinoflagellate cyst and radiolarian zonation with estimated correlation to magnetostratigraphy and planktonic foraminifer zones.

composite sections in order to recover undisturbed and complete successions marked by high sedimentation rates. Soon afterwards, the astronomical time scale was extended to the base of the Pliocene based on ODP sites (Shackleton et al., 1990) and land-based sections in the Mediterranean (Hilgen, 1991a,b), the study of the latter providing another means to overcome the problem of incompleteness of the stratigraphic record.

GTS2004 for the first time presents an Astronomically Tuned Neogene Time Scale (ATNTS2004), based on cyclic sedimentary successions from the western Equatorial Atlantic Ocean and Mediterranean. The new time scale represents a continuation of a development that led Berggren et al. (1995a) to incorporate the Pliocene and Pleistocene astrochronology of Shackleton et al. (1990) and Hilgen (1991a, b) in their Neogene time scale.

Construction of the new high-resolution Neogene time scale was made possible through:

(1) Technological and procedural improvements in deep-sea drilling of older Neogene strata,

(2) High-resolution studies of exposed marine sections in tectonically active areas where ancient seafloor has been rapidly uplifted, and

(3) Improvements in the accuracy of theoretical astronomical solutions resulting in the La2003 numerical solution.

A seafloor anomaly profile from the Australia-Antarctic plate pair was employed to complete the polarity time scale for the interval between 13 and 23 Ma due to the lack of magnetostratigraphic records for ODP Leg 154 sites. Biostratigraphic zonal schemes are either directly tied to the new time scale via first-order calibrations, such as the standard low-latitude calcareous plankton zonation, or can be linked to it by recalibrating them to the associated polarity time scale. Formally designated chronostratigraphic boundaries (GSSPs of Neogene stages) are also directly tied to the new time scale because they are defined in sections that have been used to build the astronomically tuned integrated stratigraphic framework that underlies the time scale. An overview of the tuned Neogene stratigraphic framework is in Figures 5a and b.

The new time scale resulted in a significantly younger age of 23.03 Ma for the Oligocene-Miocene boundary than the 23.8 Ma estimated in previous time scales; the latter age was based on radiometric age determinations that are not fully acceptable according to current standards. The intercalibration of the independent astronomical and radiogenic-isotopic dating methods is not yet solved, but new results (Kuiper, 2003) point to an astronomical-derived age of 28.24 ± 0.01 Ma for the Fish Canyon Tuff (FCT) sanidine and favor the introduction of a directly astronomically dated standard in $40\text{Ar}-39\text{Ar}$ dating.

The astronomically tuned Neogene time scale with an unprecedented accuracy (1–40 kyr) and resolution (<10 kyr), opens new perspectives for paleoclimatic and paleoceanographic studies of the entire Neogene with a temporal resolution comparable to that of Pleistocene research (i.e., Krijgsman et al., 1999; Zachos et al., 2001).

GTS Quo Vadis?

The changing philosophy in time scale building has made it more important to undertake high-resolution radiometric study of critical stratigraphic boundaries, and extend the astronomical tuning into progressively older sediments. Good examples are Bowring et al. (1989) for basal-Triassic, Amthor et al. (2003) for basal-Cambrian and Hilgen et al. (2000) for Messinian. The philosophy is that obtaining high-precision age dating at a precisely defined stratigraphic boundary avoids stratigraphic bias and its associated uncertainty in rock and in time.

In this respect, it is of vital importance that ICS not only completes the definition of all stage boundaries, but also actively considers definition of standardized subdivisions within the many long stages itself. Examples of long stages (spanning more than 10 myr)

that lack international standardization of internal divisions are the Campanian, Albian, Aptian, Norian, Carnian, Sakmarian, Viséan, Tournaisian, Famennian and Tremadocian stages, and parts of the Cambrian system. This consensus definition process should be completed in a timely manner. Regional and philosophical arguments between stratigraphers should be actively resolved to reach consensus conclusions which focus on the global correlation implications. Stratigraphic standardization precedes linear time calibration.

Future challenges to time scale building, detailed in Gradstein et al. (2004), may be summarized as follows:

(1) Formal definition of all Phanerozoic stage boundaries, and interior definition of long stages.

(2) Orbital tuning of polarity chrons and biostratigraphic events for the entire Cenozoic and Cretaceous (past 150 myr).

(3) A consensus Ar/Ar monitor age ($? 28.24 \pm 0.01$ Ma from orbital tuning), and consensus values for decay constants in the K-Ar isotope family.

(4) A detailed public database of high-resolution radiometric ages that includes “best practice” procedures, full error propagation, monitor ages and conversions.

(5) Resolving of zircon controversies across Devonian/Carboniferous, Permian/Triassic, and Anisian/Ladinian boundaries, either through more sampling or re-evaluation of different laboratory techniques.

(6) Detailed age dating of several ‘neglected’ intervals, including Upper Jurassic–Lower Cretaceous (M-sequence spreading and ‘tuned’ stages), base Carboniferous (Kellwasser extinction event; glaciation), and within Albian, Aptian, Norian, Carnian, Viséan, and intra Permian.

(7) More detailed composite standard zonal schemes for Upper Paleozoic and Lower Mesozoic.

(8) On-line stratigraphic databases and tools (e.g., a rapid expansion of the **CHRONOS** network).

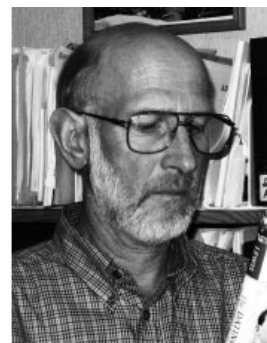
The geochronological science community and ICS are focusing on these challenging issues. The next version of the Geologic Time Scale is planned for the 33rd IGC in 2008, concurrent with the planned completion of boundary-stratotype (GSSP) definitions for all international stages.

References

- Allègre, C.J., Manhès, G., and Göpel, C., 1995, The age of the Earth; *Geochimica et Cosmochimica Acta*, 59 (8), p. 1445-1456.
- Amthor, J. E., Grotzinger, J.P., Schroder, S., Bowring, S.A., Ramezani, J., Martin, M.W., and Matter, A., 2003, Extinction of Cloudina and Namacalathus at the Precambrian boundary in Oman. *Geology*, 31 (5), p. 431-434.
- Berger, A., 1977, Long term variations of the Earth's orbital elements: *Celestial Mechanics*, 15, p. 53-74.
- Berggren, W.A., Kent, D.V., and Van Couvering, J.A., 1985, The Neogene: Part 2, Neogene geochronology and chronostratigraphy, in Snelling, N.J., ed., *The Chronology of the Geological Record: Geological Society of London Memoir* 10, p. 211-250.
- Berggren, W.A., Hilgen, F.J., Langereis, C.G., Kent, D.V., Obradovitch, J.D., Raffi, I., Raymo, M., and Shackleton, N.J., 1995, Late Neogene (Pliocene-Pleistocene) chronology: New perspectives in high-resolution stratigraphy: *Geological Society of America Bulletin*, 107, p. 1272-1287.
- Blake, T.S., and Groves, D.I., 1987, Continental rifting and the Archean-Proterozoic transition. *Geology*, 15, p. 229-232.
- Bleeker, W., 2003a, Problems with the Precambrian timescale: from accretion to Paleoproterozoic plate break-up. See <http://www.nunatime.ca>.
- Bleeker, W., 2003b, The late Archean record: a puzzle in ca. 35 pieces. *Lithos*, 71 (2/4), p. 99-134.
- Bowring, S.A., Ramezani, J., and Grotzinger, J.P., 2003, High-precision U-Pb zircon geochronology and Cambrian-Precambrian boundary. See <http://www.nunatime.ca>.
- Cande, S.C., and Kent, D.V., 1992, A new geomagnetic polarity time scale for the Late Cretaceous and Cenozoic. *Journal of Geophysical Research*, 97, p. 13917-13951.
- Cande, S.C. and Kent, D.V., 1995, Revised calibration of the geomagnetic polarity timescale for the Late Cretaceous and Cenozoic. *Journal of Geophysical Research*, 100, p. 6093-6095.

- Cloud, P., 1972, A working model of the primitive Earth. *American Journal of Science*, 272, p. 537-548.
- Cloud, P., 1987, Trends, transitions, and events in Cryptozoic history and their calibration: apropos recommendations by the Subcommittee on Precambrian Stratigraphy. *Precambrian Research*, 37, p. 257-264.
- Cooper, R.A., 1999, The Ordovician time scale - calibration of graptolite and conodont zones: *Acta Universitatis Carolinae Geologica*, 43 (1/2), p. 1-4.
- Crook, K.A.W., 1989, Why the Precambrian time-scale should be chronostratigraphic: a response to recommendations by the Subcommittee on Precambrian Stratigraphy. *Precambrian Research*, 43, p. 143-150.
- Gradstein, F.M., Agterberg, F.P., Ogg, J.G., Hardenbol, J., van Veen, P., Thierry, T., and Huang, Z., 1994, A Mesozoic time scale. *Journal of Geophysical Research*, 99 (B12), p. 24051-24074.
- Gradstein, F.M., Ogg, J.G., Smith, A.G., Agterberg, F.P., Bleeker, W., Cooper, R.A., Davydov, V., Gibbard, P., Hinnov, L.A., House, M.R. (†), Lourens, L., Luterbacher, H-P., McArthur, J., Melchin, M.J., Robb, L.J., Shergold, J., Villeneuve, M., Wardlaw, B.R., Ali, J., Brinkhuis, H., Hilgen, F.J., Hooker, J., Howarth, R.J., Knoll, A.H., Laskar, J., Monechi, S., Powell, J., Plumb, K.A., Raffi, I., Röhl, U., Sanfilippo, A., Schmitz, B., Shackleton, N.J., Shields, G.A., Strauss, H., Van Dam, J., Veizer, J., van Kolschoten, Th., and Wilson, D., 2004 (in press), *A Geologic Time Scale 2004*. Cambridge University Press, ~500 pp
- Guest, J.E., and Greeley, R., 1977, *Geology on the Moon*; The Wykeham Science Series, Crane, Russak and Company, Inc., New York, 235 pp.
- Harland, W.B., Cox, A.V., Llewellyn, P. G., Pickton, C.A.G., Smith, A.G., and Walters, R., 1982, *A geologic time scale 1982*, Cambridge University Press, 131 pp.
- Harland, W.B., Armstrong, R.L., Cox, A.V., Craig, L.E., Smith, A.G., and Smith, D.G., 1990, *A geologic time scale 1989*. Cambridge University Press, 263 pp.
- Heirtzler, J.R., Dickson, G.O., Herron, E.M., Pitman, W.C., and Le Pichon, X., 1968, Marine magnetic anomalies, geomagnetic field reversals, and motions of the ocean floor and continents. *Journal of Geophysical Research*, 73, p. 2119-2139.
- Hilgen, F.J., 1991a, Extension of the astronomically calibrated (polarity) time scale to the Miocene/Pliocene boundary. *Earth and Planetary Science Letters*, 107, p. 349-368.
- Hilgen, F.J., 1991b, Extension of the astronomically calibrated (polarity) time scale to the Miocene-Pliocene boundary. *Earth and Planetary Science Letters*, 107, p. 349-368.
- Hilgen, F.J., Krijgsman, W., Langereis, C.G., Lourens, L.J., Santarelli, A., and Zachariasse, W.J., 1995, Extending the astronomical (polarity) time scale into the Miocene. *Earth and Planetary Science Letters*, 136, p. 495-510.
- Hilgen, F.J., Bissoli, L., Iaccarino, S., Krijgsman, Meijer, R., Negri, A., and Villa, 2000, Integrated stratigraphy and astrochronology of the Messinian GSSG at Oued Akrech (Atlantic Morocco). *Earth and Planetary Science Letters*, 182, p. 237-251.
- Holmes, A., 1947, The construction of a geological time-scale. *Transactions Geological Society of Glasgow*, 21, p. 117-152.
- Holmes, A., 1960, A revised geological time-scale. *Transactions of the Edinburgh Geological Society*, 17, p. 183-216.
- Krijgsman, W., Hilgen, F.J., Raffi, I., Siero, F.J., and Wilson, D.S., 1999, Chronology, causes and progression of the Messinian salinity crisis: *Nature*, 400, p. 652-655.
- Kuiper, K.F., 2003, Direct intercalibration of radio-isotopic and astronomical time in the Mediterranean Neogene: *Geologica Ultraiectina (Mededelingen van de Faculteit Geowetenschappen, Universiteit Utrecht)*, 235, 223 pp.
- Ludwig, K.R., 2000, Decay constant errors in U-Pb Concordia-intercept ages. *Chemical Geology*, 166, p. 315-318.
- Lumbers, S.B., and Card, K.D., 1991, Chronometric subdivision of the Archean. *Geology*, 20, p. 56-57.
- Murray, B., Malin, M.C., and Greeley, R., 1981, *Earthlike planets; surfaces of Mercury, Venus, Earth, Moon, Mars*; W.H. Freeman and Company, San Francisco, 387 pp.
- Nisbet, E.G., 1991, Of clocks and rocks—The four aeons of Earth. *Episodes*, 14, p. 327-331.
- NUNA, 2003, *New Frontiers in the fourth dimension: generation, calibration and application of geological timescales*; NUNA Conference, Geological Association of Canada; Mont Tremblant, Quebec, Canada, March 15-18, 2003. See <http://www.nunatime.ca>.
- Obradovich, J.D., 1993, A Cretaceous time scale, in Caldwell, W.G.E., and Kauffman, E.G., eds., *Evolution of the Western Interior Basin*, Geological Association of Canada, Special Paper 39, p. 379-396.
- Plumb, K.A., 1991, New Precambrian time scale. *Episodes*, 14, p. 139-140.
- Plumb, K.A., and James, H.L., 1986, Subdivision of Precambrian time: Recommendations and suggestions by the commission on Precambrian stratigraphy. *Precambrian Research*, 32, p. 65-92.
- Remane, J., 2000, *International Stratigraphic Chart, with Explanatory Note*. Sponsored by ICS, IUGS and UNESCO. (distributed at the 31st International Geological Congress, Rio de Janeiro 2000), 16 pp.
- Shackleton, N.J., Berger, A., and Peltier, W.R., 1990, An alternative astronomical calibration of the lower Pleistocene timescale based on ODP site 677. *Transactions of the Royal Society of Edinburgh*, 81, p. 251-261.
- Shackleton, N.J., Crowhurst, S.J., Weedon, G.P., and Laskar, J., 1999, Astronomical calibration of Oligocene-Miocene time. *Philosophical Transactions of the Royal Society of London, A*, (357), p. 1907-1929.
- Spudis, P.D., 1999, *The Moon*. In: *The New Solar System*, edited by J.K. Beatty, C. Collins Petersen and A. Chaikin, Cambridge University Press, Cambridge, p. 125-140.
- Trendall, A.F., 1991, The "geological unit" (g.u.)—A suggested new measure of geologic time. *Geology*, 19, p. 195.
- Windley, B.F., 1984, The Archaean-Proterozoic boundary. *Tectonophysics*, 105, 43-53.
- Zachos, J., Pagani, M., Sloan, L., Thomas, E., and Billups, K., 2001, Trends, rhythms, and aberrations in global climate 65 Ma to present. *Science*, 292, p. 686-693.

Felix M. Gradstein is chair of the International Commission on Stratigraphy. Following retirement from the Geological Survey of Canada and Saga Petroleum Norway, he joined the Natural History Museum, University of Oslo as stratigraphy/micropaleontology professor, where he is developing relational stratigraphic databases for offshore Norway. His activities have included quantitative stratigraphy (he chaired previous IGCP and IUGS programs), Ocean Drilling Program legs in the Atlantic and Indian oceans, and coordinating compilation of Mesozoic and Phanerozoic geologic time scales. He is an avid skier and offshore sailor.



Jim Ogg, a professor of stratigraphy at Purdue University in Indiana USA, has been serving as Secretary-General of the International Commission on Stratigraphy of IUGS since 2000. His research concentrates on the Mesozoic and Paleogene, especially paleoceanography (including ten DSDP-ODP drilling cruises), time scales of cyclic sedimentation and magnetic polarity chrons, and integrated Earth history. Gabi Ogg, his wife and fellow stratigrapher, was responsible for most of the graphics on the ICS website and in the GTS2004 book.

